



# New Absolute Cavity Radiometer equation by application of Kirchhoff's law and adding a convection term

Bruce W. Forgan<sup>1</sup>, Julian Gröbner<sup>2</sup>, Ibrahim Reda<sup>3</sup>

<sup>1</sup>Docklands, Victoria, 3008, Australia

5 <sup>2</sup>PMOD/WRC, Davos Dorf, 7260, Switzerland

<sup>3</sup>NREL, Golden, Colorado, 80401-3393, USA

*Correspondence to:* Bruce W. Forgan (bwforgan@bigpond.com)

**Abstract.** An equation for the Absolute Cavity Pyrgeometer (ACP) is derived from application of Kirchhoff's law and the addition of a convection term to account for the thermopile being open to the environment unlike a domed radiometer. The equation is then used to investigate four methods to characterise key instrumental parameters using laboratory and field measurements. The first uses solar irradiance to estimate the thermopile responsivity, the second a minimisation method that solves for the thermopile responsivity and transmission of the cavity, and the third and fourth revisit the Reda et. al., 2012 linear least squares calibration technique. Data were collected between January and November 2020 when the ACP96 and two IRIS radiometers monitoring terrestrial irradiances were available. The results indicate good agreement with IRIS irradiances using the new equation. The analysis also indicates that while the thermopile responsivity, concentrator transmission and emissivity of an ACP can be determined independently, as an open instrument, the impact of the convection term is minor in steady state conditions but significant when the base of the instrument is being subjected to rapid artificial cooling or heating. Using laboratory characterisation of the transmission and emissivity, together with use of an estimated solar calibration of the thermopile generated mean differences of less than  $1.5 \text{ Wm}^{-2}$  to the two IRIS radiometers. The minimization method using each IRIS radiometer as the reference also provided similar results, and the derived thermopile responsivity was within  $0.3 \mu\text{V/Wm}^{-2}$  of the solar calibration derived infrared responsivity estimate of  $10.5 \mu\text{V/Wm}^{-2}$  estimated using a nominal solar calibration and within  $\pm 2\%$  of the terrestrial irradiance measured by the reference pyrgeometers traceable to SI. The calibration method using linear least squares regression introduced by Reda et al., 2012 that relies on rapid cooling of the ACP base but utilising the new equation was found to produce consistent results but was dependent on the analogue used for temperature of air above the thermopile. The result of this study demonstrates the potential of the ACP as another independent reference radiometer for terrestrial irradiance once the impact of convection on the ACP has been resolved.

## 1 Background

Reda et al., 2012 introduced the Absolute Cavity Radiometer (ACP), its operational equations and characterization process. The ACP is an Eppley Laboratory pyrgeometer (PIR) with its dome replaced by a symmetrical cavity (called the concentrator)



30 internally coated by polished gold, and a cooling apparatus attached to the base of the pyrgeometer to assist in cooling or heating the ACP body.

The Reda et al., 2012 derivation of the ACP equation uses a combination of radiative transfer but without consideration of reflected irradiance components and impacts of convection (Vignola et al., 2012). Blackbody calibration of an ACP has proven difficult and Reda et al., 2012 proposed a method of characterisation and calibration that included laboratory methods to  
35 determine the transmission of the concentrator and the emissivity of polished gold, while the thermopile sensitivity is determined using a linear least squares regression (LSQ) technique in the field at night under stable incoming irradiance conditions. Calibrations provided by Reda et al., 2012 assumed that the responsivity and transmission of the ACP changes over hours and days with variations of the order of several percent. More recently, Gröbner, 2021 has shown that the selection of points used in the field calibration have a significant influence on the result.

40 The ACP's body uses a Eppley Laboratory F3 thermopile which is used for Eppley Laboratory pyranometers (PSP) and pyrgeometers (PIR). The stability of F3 thermopile for solar and infrared irradiance measurements using domed instruments is well within a percent over several years. Therefore, it was surprising to see the large variation in the ACP thermopile responsivity ( $\mu\text{V}/(\text{Wm}^{-2})$ ) reported by Reda et al., 2012.

This paper derives a new ACP equation that adheres to Kirchhoff's law of thermal radiation for radiative transfer in vacuum  
45 and in-air measurements with a thermopile not protected by a dome and therefore includes an energy transfer term due to convection. The similarity and key differences in the contributing terms of the new in-air and the Reda et al., 2012 equations are also examined. Using the new equation, the impact on the laboratory characterisation, night-time calibration compared against two IRIS pyrgeometers, and an application of the linear LSQ methods are investigated.

## 2 The steady-state equation for an ACP without a dome or concentrator in a vacuum

50 An ACP without a concentrator is an Eppley Laboratory pyrgeometer without a dome that includes a thermistor to measure the temperature of the body. It has a flat thermopile receiver painted with Parsons Black. In a vacuum there is only radiative transfer between the source and the thermopile receiver, with no possibility of a convection component.

The ACP equation in this instance only involves Kirchhoff's law at the black surface of the thermopile receiver namely  
$$1 = \alpha_r + \rho_r \tag{1}$$

55 where  $\alpha_r$  is the fraction absorbed by the receiver which from Kirchhoff's law is equivalent to emissivity  $\epsilon_r$  and  $\rho_r$  is the fraction reflected from the receiver as there is no transmission through the black receiver surface.

The net flux between the incoming and outgoing flux results in a temperature difference between the base and receiver of the thermopile generating a voltage that is proportional to the net flux. That is,  
$$KV = F \downarrow - F \uparrow \tag{2}$$



60 where  $K$  is the responsivity of the thermopile in  $\text{Wm}^{-2}\mu\text{V}^{-1}$ ,  $V$  is the voltage and  $F\downarrow$  and  $F\uparrow$  are the downward and upward radiant fluxes. The downward flux is made up of a single component the irradiance from the source  $W$ ,

$$F\downarrow = W \quad (3)$$

The upward flux has two components, the emission from the surface and the reflection of the incoming flux, that is,

$$F\uparrow = \varepsilon_r W_r + (1 - \varepsilon_r) F\downarrow \quad (4)$$

65 where  $\varepsilon_r$  is the emissivity of the receiver, and  $W_r$  is the blackbody irradiance from the receiver;  $\rho_r$  is equal to  $(1 - \varepsilon_r)$  as there is no transmission through the receiver surface. Solving the two simultaneous equations the result is

$$KV = F\downarrow - F\uparrow = W - W_r \varepsilon_r \quad (5)$$

which gives for  $W$

$$W = \frac{K}{\varepsilon_r} V + W_r = K_r V + W_r \quad (6)$$

70 where  $K_r$  is the responsivity of the thermopile receiver or  $K_r = K/\varepsilon_r$ .

$W_r$  is given by  $\sigma T_r^4$ . As  $T_r$  cannot be measured directly at time  $t$  it is approximated by

$$T_r(t) = T_{rb}(t) + V(t)S \quad (7)$$

where  $T_b$  is the ACP body temperature,  $S$  is calculated based on known values of the Seebeck coefficient for the thermopile junctions. If  $n$  is the number of junctions and  $\varpi$  is the efficiency of the thermopile, then

$$75 \quad S = \frac{1}{S_0 n \varpi} \quad (8)$$

For the Eppley Laboratory F3 thermopile used in an ACP, with 56 copper-constantan junctions,  $S_0$  is  $\sim 40 \mu\text{V/K}$ , and Reda et al., 2012 suggested  $\varpi \sim 0.65$  or 65% efficiency.  $(T_r - T_b)$  is dependent on the net incoming irradiance and the thermal conductivity of the thermopile, while  $S$  is a property solely of the thermopile, and impacts directly on the thermopile responsivity.  $\varpi$  may vary due to the manufacturing process. During operation of an ACP the maximum expected  $(T_r - T_b)$  is about 0.7 K. Reda et al., 80 2012 proposed  $S$  to be  $7.044 \cdot 10^{-4}$ . For a  $T_b = 273.15 \text{ K}$ , and steady state conditions where  $V \sim 800 \mu\text{V}$  (corresponding to the net radiation exchange of the ACP with a cloud free sky), if  $S$  is in error by 20% the impact on  $W_r$  is about  $0.7 \text{ Wm}^{-2}$  and increases proportionally with  $V$  and  $T_b$ .

### 3 The steady-state equation of an ACP with a symmetrical concentrator in a vacuum

The concentrator is assumed to have symmetrical transmission, absorption, and backscatter characteristics. That is,

$$85 \quad 1 = \tau + \beta + \alpha \quad (9)$$



where  $\tau$  is the transmitted fraction of the incoming irradiance through the concentrator,  $\alpha$  is the fraction of the incoming irradiance absorbed by the concentrator and  $\beta$  is the fraction of the incoming irradiance reflected out of the concentrator. Being a symmetrical cavity, each component's magnitude will remain the same if irradiance enters either end of the concentrator.

The concentrator walls coated in gold have an emissivity (or absorptivity) of  $\varepsilon_c$  that is a property of the surface and independent of the incoming irradiance. The fraction of incoming irradiance absorbed by the concentrator,  $\alpha$ , is a consequence of  $\varepsilon_c$  and the scattering of incoming irradiance on the concentrator walls.

For an ACP in a vacuum, the incoming flux  $F \downarrow$  at the receiver (at one end of the symmetrical concentrator) has three components, the transmitted incoming atmospheric irradiance  $\tau W$ , any emission from the walls of the concentrator with a blackbody irradiance of  $W_c$ ,  $\varepsilon_c W_c$ , and the back reflectance towards the receiver of the flux from the receiver  $\beta F \uparrow$  that is,

$$95 \quad F \downarrow = \tau W + \varepsilon_c W_c + \beta F \uparrow \quad (10)$$

The outgoing flux from the receiver is made up of two components, namely the emitted irradiance from the receiver and the reflected incoming flux, that is,

$$F \uparrow = W_r \varepsilon_r + (1 - \varepsilon_r) F \downarrow \quad (11)$$

Solving the two simultaneous equations results in

$$100 \quad KV = F \downarrow - F \uparrow = \frac{\varepsilon_r(\tau W + \varepsilon_c W_c - (1 - \beta)W_r)}{1 - \beta(1 - \varepsilon_r)} \quad (12)$$

As a result, the incoming irradiance transmitted by the concentrator is

$$\tau W = \frac{(1 - \beta(1 - \varepsilon_r)K)}{\varepsilon_r} V + (1 - \beta)W_r - \varepsilon_c W_c \quad (13)$$

And the required irradiance is

$$W = \frac{(1 - \beta(1 - \varepsilon_r)K)}{\varepsilon_r \tau} V + \frac{(1 - \beta)}{\tau} W_r - \frac{\varepsilon_c}{\tau} W_c \quad (14)$$

105 Note that Eq. (14) would be similar to the domed pyrgeometer equation by Philipona et al., 1996 if the latter used  $T_r$  instead of the thermopile base temperature, and the transmission and emission is that of a dome instead of an open cavity.

#### 4 The steady-state equation of an ACP with a symmetrical concentrator in the atmosphere

In air, as the concentrator is open to the atmosphere, and convection effects are not minimized by a dome (Robinson, 1966, Kondratyev, 1969, Vignola et al., 2012), a convection term is required. The effective flux input to the receiver by convection is given by

$$F_{conv} = \gamma(T_{air} - T_r) \quad (15)$$

where  $\gamma$  is the convection coefficient dependent on several factors such as water vapour content, wind speed and air pressure



(Vignola et al., 2012), and  $T_{air}$  the temperature of the air at the surface of the receiver. The equivalent version of equation (10) is,

$$115 \quad F \downarrow = \tau W_{atm} + \varepsilon_c W_c + \beta F \uparrow + \gamma(T_{air} - T_r) \quad (16)$$

The outgoing flux from the receiver is made up of two components, identical to Eq. 11.

Solving the two simultaneous equations results in

$$\tau W_{atm} = \frac{(1-\beta(1-\varepsilon_r))K}{\varepsilon_r} V + (1-\beta)W_r - \varepsilon_c W_c + \gamma(T_r - T_{air}) \quad (17)$$

and replacing  $K/\varepsilon_r$  with  $K_1$  the atmospheric irradiance is

$$120 \quad W_{atm} = \frac{K_1}{\tau} V + \frac{(1-\beta)}{\tau} W_r - \frac{\varepsilon_c}{\tau} W_c + \frac{\gamma}{\tau} (T_r - T_{air}) = \frac{K_1}{\tau} V + W_{net} \quad (18)$$

where  $W_{net}$  represents the non-voltage irradiance components, and

$$K_1 = \frac{(1-\beta(1-\varepsilon_r))}{\varepsilon_r} K = \frac{1}{C}$$

and  $C$  is the effective responsivity of the thermopile receiver in  $\mu V/(Wm^{-2})$ . The only difference between Eq. (14) and Eq. (18) is the convection term  $F_{conv}$ . In a domed radiometer, as the sensor surface and air under the dome are at near equilibrium, the effects of convection are minimized and their inclusion in the flux balance of the thermopile is not used.

125

As there is no direct measure of the air temperature in the concentrator near the receiver surface, Reda et al., 2012 averaged the 6 temperature sensors embedded in the concentrator  $T_c$  to represent  $T_{air}$ .

## 5 Examining the laboratory determined coefficients

The emissivity of the polished gold-plated concentrator in APC95 was found by NIST measurements to be 0.0225. The transmission of the concentrator was investigated by Jinan et al., 2010 via

130

$$\tau = \frac{(V_c K_1 + W_{rc})}{S_c} / \frac{(V_o K_1 + W_{ro})}{S_o} \quad (19)$$

with subscripts  $o$  and  $c$  representing ACP measurements with the concentrator removed and with the concentrator in-place.  $S_c$  and  $S_o$  are the reference output signals of the irradiance source; the derived value was 0.92. Reda et al., 2012 indicated that the  $K_1$  value used by Jinan et al., 2010 was incorrect and used a value  $K_1 \sim 0.080 \mu V Wm^{-2} \mu V^{-1}$  (or  $C \sim 12.5 \mu V/(Wm^{-2})$ ) from field calibrations to generate a  $\tau \sim 0.993$ .

135

As these measurements were conducted in air, Eq. (18) applies and hence a convection term and concentrator emission term should have been added to the concentrator term in the numerator and the denominator namely,



$$\tau = \frac{(V_c K_1 + W_r c - \varepsilon_c W_{cc} + \gamma(T_r c - T_{air} c))}{S_c} / \frac{(V_0 K_1 + W_{r0} + \gamma(T_{r0} - T_{air0}))}{S_0} \quad (20)$$

The laboratory setup used by Jinan et al., 2010 included a 10  $\mu\text{m}$  laser and its irradiance was higher than the irradiance from base of the ACP, hence positive signals resulted from the ACP thermopile and  $T_r$  would have been higher than  $T_c$ . Setting  $\beta \sim 0$ ,  $\varepsilon_c = 0.0225$ , and  $\gamma \sim 8.5$  and assuming the thermopile to air temperature difference was about +0.3 K in steady state conditions resulted in 1.5% reduction in the transmission to  $\sim 0.977$  when compared to the values used in Reda et al., 2012. The impact of a zero contribution from the convection term decreased the derived transmission by less than 0.001.

Reda et al., 2012 utilised Eq. (19) and the results from Jinan et al., 2010 to derive a value of  $\tau$  for each measurement sequence after updating  $K_l$  via a linear LSQ calibration run. As a result,  $\tau$  was deemed a function of  $K_l$ , rather than a unique characteristic of the concentrator.

## 6 Comparing the terms between the original and new ACP equations

Using the symbols above, the Reda et al., 2012 equation for incoming irradiance is

$$W_{atm} = \frac{K_1}{\tau} V + \frac{(2 - \varepsilon_c)}{\tau} W_r - \frac{(\varepsilon_c + \varepsilon_{cav})}{\tau} W_c \quad (21)$$

with the only additional term being the emissivity of the air in the cavity  $\varepsilon_{cav}$  which Reda et al., 2012 set to 1. Rearranging the terms, we have

$$W_{atm} = \frac{K_1}{\tau} V + \frac{1}{\tau} W_r - \frac{\varepsilon_c}{\tau} W_c + \frac{1}{\tau} (W_r - W_c) - \frac{\varepsilon_c}{\tau} W_r \quad (22)$$

The first 3 terms of Eq. (18) and Eq. (22) are identical if the backscatter  $\beta$  is zero. The latter two terms are where significant differences to the new equation exist. The  $(W_r - W_c)$  term is a difference between irradiances rather than a difference in temperatures in Eq. (18). In steady state conditions with the base of the ACP not subject to artificial cooling or heating,  $W_r \leq W_c$  and  $-0.6 < (T_r - T_c) \leq 0.0$ , there is a relatively simple relationship between the irradiance difference and the temperature difference, namely

$$(W_r - W_c) \sim \psi(T_r - T_c) \quad (23)$$

where  $\psi \cong 5 \pm 2$  depending on the usual range of irradiance terms. The magnitude of  $\gamma$  from black body investigations using ACP96 is  $\gamma \sim 8.4$  and  $6.5$  depending on the blackbody configuration and are higher than  $\psi$ . In essence, the  $(W_r - W_c)$  is a lower magnitude version of the convection term in the new equation. The last term in Eq. (22), namely  $-W_r \varepsilon_c / \tau$  adds a negative irradiance contribution due to the concentrator emissivity but sourced from the thermopile irradiance; this is not consistent with Kirchhoff's law as it adds emission from the concentrator walls other than due to the concentrator's temperature.



Hence the only differences between Eq. (22) and Eq. (18) are that for Eq. (22):  
165 (a) the  $\varepsilon_c/\tau$  terms have approximately double the contribution to the derived atmospheric irradiance; and  
(b) the  $(W_r - W_c)$  term could be slightly less in magnitude compared to the  $\gamma(T_r - T_c)$ .

The doubling of the  $\varepsilon_c/\tau$  contribution in Eq. (22) impacts directly on any derivation of  $K_1$  as it increases the negative  
contributions from both the concentrator and thermopile irradiance emission. That is, given  $V$  is normally negative and as the  
concentrator emissivity  $\varepsilon_c$  is a constant, the Reda et al., 2012 derived  $K_1$  will be smaller (and hence  $C$  is larger) compared to  
170 Eq. (18) derivations by about 8%.

### 7 ACP calibration methods to date

As the ACP was developed to be an absolute radiometer that did not require calibration through comparison to another  
pyrgeometer or black body source, Reda et al., 2012 developed an innovative calibration method using linear LSQ that relies  
on periods of constant  $W_{atm}$  together with rapid changes in the thermopile base temperature. The base and concentrator  
175 temperature providing irradiance traceability to SI. As the calibration process rapidly and continuously drops the base  
temperature of the ACP the changes in signals and component irradiances are used to generate a linear LSQ solution. Two  
parameters are derived from the linear LSQ calibration process,  $\langle K_I \rangle$  and  $\langle \tau W_{atm} \rangle$ . For Reda et al., 2012  $\varepsilon_c$  and  $\varepsilon_{cav}$  coefficients  
in Eq. (22) are based on laboratory measurements or assumptions from literature.

During the Reda et al., 2012 linear LSQ process the ACP body is rapidly cooled over a set period. The rapid change in base  
180 temperature is required to minimize the risk that  $W_{atm}$  changes significantly over the cooling period. The measurements during  
the rapid heating after a cooling process are not used.

Using ACP96 data Gröbner, 2021 examined the linear LSQ process and developed procedures to remove the influence of the  
initial and final transient values and only used those data where a continuous cooling process is evident. Using Eq. (22) these  
results implied data selection generates  $\langle K_I \rangle$  that are approximately 6% less than the Reda et al., 2012 implementation. This  
185 suggests the difference between the results from Reda et al., 2012 and the use Eq. (18) could be about 14%. The average value  
for  $\langle K_I \rangle$  in Reda et al., 2012 is  $\sim 0.080$ , so using the linear LSQ methodology with Eq. (18) should likely produce a value of  
about 0.091 or  $C \sim 10.9 \mu\text{V}/(\text{Wm}^{-2})$  for the same ACP.

Black body methods have been used successfully for decades to calibrate domed pyrgeometers and solving for Eq. (14)  
equivalents that have shown high levels of stability over several years (Gröbner and Wacker, 2012). In black body calibrations  
190 of a pyrgeometer, the base temperature of the pyrgeometer, and its dome, and the blackbody output irradiance are changed and  
allowed to stabilize at set values. The number of different plateau settings of these variables allows a multivariate solution by  
LSQ optimization methods. However, the final determination of  $K_I$  is typically by using dome irradiance coefficients derived



from the black body calibration together with a reference irradiance during night-time measurements (Gröbner and Walker, 2012).

195 Black body methodologies have not been successful for calibration of an ACP to date. The only differences between a typical pyrgeometer and ACP are the replacement of a dome with the open concentrator, and the careful matching of the thermistors with the latter an improvement on normal pyrgeometer thermometry; the most significant difference is that the ACP thermopile and concentrator aperture is open to the environment. The black body calibration process used for pyrgeometers requires a fixed number of temperature and black body stable points sufficient to solve for 3 unknowns instead of 4. Hence one issue  
200 with blackbody calibration of an ACP could be that the number of stable points used in the multivariate LSQ solution for an ACP is insufficient. However, given the concentrator is open to the air in the black body, the assumption that the air temperature in the concentrator is very close to the concentrator temperature is likely to be incorrect.

### 7.1 The impact of uncertainty in concentrator, thermopile and convection coefficients on $W_{atm}$

Using the new equation, the concentrator properties are the concentrator transmission  $\tau$ , its emissivity  $\varepsilon_c$ , the concentrator  
205 backscatter  $\beta$  and the remainder or absorptivity of the incoming irradiance  $\alpha_c$ ; the contributing thermopile property is its emissivity  $\varepsilon_r$ , and the convection term is  $\gamma$ .  $\alpha_c$  is not required but given Kirchhoff's law indicates it would not be independent of  $\varepsilon_c$ .

A value for the thermopile emissivity  $\varepsilon_r$  is not required as it is a constant and it is incorporated in  $K_1$  (and  $C$ ). For Parsons  
Black at terrestrial irradiance wavelength  $\varepsilon_r$  is  $\sim 0.92$  and at solar wavelengths  $\sim 0.98$ .  $\varepsilon_r$  only becomes relevant if  $C$  is determined  
210 at solar wavelengths ( $C_{solar}$ ), and then converted to a terrestrial irradiance value, as we will see below.

For ACP95 the concentrator emissivity was measured by NIST (Reda et al., 2012) and was found to be 0.0225 which is within 0.0015 of other known values for the emissivity (and hence absorptivity) of polished gold. Given that  $W_c$  is between 300 and 500  $\text{Wm}^{-2}$  for most measurement locations, and the NIST laboratory measurements estimates of concentrator transmission  $\tau > 0.9$  the likely maximum impact on  $W_{atm}$  of an incorrect assignment of the  $\varepsilon_c/\tau$  coefficient is less than 2.5  $\text{Wm}^{-2}$ .

215 The impact of the irradiance backscatter fraction  $\beta$  and the receiver emissivity  $\varepsilon_r$  is minimal. The Jinan et al., 2010 transmission measurements and using in the new equation suggest that for a concentrator transmission  $\tau$  greater than 0.9, and as  $(1-\tau) \geq \beta$  and  $\varepsilon_r > 0.9$ , then  $(1-\beta(1-\varepsilon_r)) \geq 0.99$  and are essentially constant hence they have little impact and easily incorporated into  $K_1$ .

The greatest potential impact due to concentrator transmission  $\tau$  and backscatter  $\beta$  is on the  $W_r$  term where  $1.1 \geq (1-\beta)/\tau > 1.0$  when the fraction of incoming irradiance  $\alpha_c$  is greater than zero. If there is no absorption of the incoming irradiance by the  
220 concentrator (i.e.  $\alpha_c=0$ ) then  $(1-\beta)$  is equal to  $\tau$ . If  $\alpha_c > 0$  and  $(1-\beta)/\tau$  is in error by 0.02 then the typical error in the  $W_r$  contribution will be between 6 and 10  $\text{Wm}^{-2}$ . As  $\beta$  is near zero, any error in concentrator transmission will dominate the error contribution to  $W_r$  and hence  $W_{atm}$ .





225 The convection coefficient  $\gamma$  is problematic for several reasons. Firstly, at present it needs to be derived assuming the other coefficients or by approximation. Secondly it is dependent on the air flow, water content and air pressure at the surface of the thermopile receiver. The empirical evidence from blackbody and atmospheric measurements suggests  $6 < \gamma < 10$ .

230 The receiver temperature  $T_r$  and hence blackbody irradiance  $W_r$  are dependent on the estimate of the Seebeck coefficient and the construction of the thermopile and the measurement of the base temperature  $T_b$ . As the thermistors in an ACP have been characterised, Reda et al., 2012 estimated that the standard uncertainty in the  $W_r$  and  $W_c$  at about  $0.1 \text{ Wm}^{-2}$  and the standard uncertainty in the estimation of the Seebeck coefficient for the thermopile provides an additional  $0.1 \text{ Wm}^{-2}$  uncertainty contribution to  $W_r$ .

235  $T_r$  is calculated using equation (7) on the assumption that the efficiency of the thermopile is as stated in Reda et al., 2012 and  $T_b$  is equivalent to the thermopile base temperature.  $K$  is also dependent on the Seebeck coefficient of the copper-constantan, the efficiency of the thermopile, the emissivity of the receiver surface  $\varepsilon_r$  and the conductivity of the thermopile. Incorrect assignment of the true Seebeck coefficient  $S$  in Eq. (7) will impact on two terms in Eqs. (18) and (22). However,  $S$  has not been derived for individual ACP, so the Reda et al., 2012 value will be assumed for this paper.

For solar wavelengths the emissivity of Parson's Black changes as the paint discolours over time due to solarization but has little if any impact on the IR emissivity.

240 The denominator of Eqs. (18) and (22) is the concentrator transmission  $\tau$  and hence a percentage change in its value has the same impact on  $W_{atm}$  through every irradiance component regardless of the equation used. It is essential for any calibration that  $\tau$  has a low uncertainty.

## 8 New Calibration Methods

Four calibration methods will be examined below for ACP96 based at PMOD/WRC in Davos, Switzerland, using either characterisation data, comparison measurements with other reference pyrgeometers, and implementing two versions of the linear LSQ method.

245 Based on the likely magnitude of the impact of the uncertainties, assumed values for some parameters are used in all the calibration methods investigated below. The value of the cavity emissivity is fixed at 0.0225 using the NIST derived value in Reda et al., 2012 for ACP95. The value for the backscatter from the concentrator  $\beta$  will be assumed to be insignificant, but  $\alpha_c$  the absorption fraction of incoming atmospheric irradiance by the concentrator will be assumed to be greater than zero and hence  $(1 - \alpha_c)$  will be greater than or equal to the concentrator transmission  $\tau$ .

250 In steady state conditions the difference between the thermopile and cavity air temperature is less than 0.5 K and in low wind conditions the temperature difference in the thermopile surface and the concentrator or air temperature is small, the impact of



a 25% error in convection coefficient  $\gamma=10$  will be less than  $1.2 \text{ Wm}^{-2}$ . Using a black body, values of the convection coefficient  $\gamma$  divided by concentrator transmission of 8.54 and 6.6 have resulted hence these two  $\gamma$  values are used below namely, 8.4 and 6.5. The latter value 6.5 derived from early blackbody investigations and field measurements produces convection-based irradiances closer to the equivalent ‘air cavity’ irradiance values used by Reda et al., 2012. The logic behind this adjustment is not solely due to the convection coefficient being different, but rather the approximation  $T_c \sim T_{air}$ . There is evidence from the concentrator temperature sensor data that during the rapid cooling of the ACP base for linear LSQ calibrations, temperatures of the three top concentrator sensors decrease at a slower rate than the sensors near the thermopile. Hence it seems likely the representative air temperature near the sensor maybe lower than the average of the 6 sensors to provide  $T_c$ ; and given the thermal capacity of the concentrator even the lowest of the  $T_c$  values may not represent  $T_{air}$  which is also exposed to the air circulating from the base of the ACP.

This leaves the sensitivity of the thermopile  $K_I$  and the concentrator transmission  $\tau$  to be either assumed or provided by a characterisation methodology.

For work reported below the transmission of the concentrator  $\tau$  is assumed to be only due to the construction of the concentrator and is independent of  $K_I$ . The values of  $\tau$  for ACP95 derived by the reanalysis of the Jinan et. al. (2010) data set but using Eq. (20) will be used when not derived as part of a calibration process.

The assumption that concentrator emissivity  $\varepsilon_c$  is independent of fraction of incoming irradiance absorbed by the concentrator  $\alpha_c$  is reconsidered for this paper. Concentrator transmission is a function of the cosine response of the concentrator and ray tracing suggests that for most sky zenith angles there will be multiple reflections on its surface, and that absorptivity is equivalent to  $\varepsilon_c$ . Hence for this paper it is assumed that concentrator transmission  $\tau$  is less than or equal to  $(1-\varepsilon_c)$ . For  $\varepsilon_c=0.0225$  derived by NIST as reported by Reda et al., 2012, then assuming  $\varepsilon_c < \alpha_c + \beta$  this implies  $\tau \leq 0.9775$ .

For the results below when the method requires a fixed value of concentrator transmission  $\tau$  is set to 0.977, and a fixed estimate of  $\varepsilon_c = 0.0225$  and two values of the convection coefficient  $\gamma$  (8.4 and 6.5).

## 8.1 Data Sets

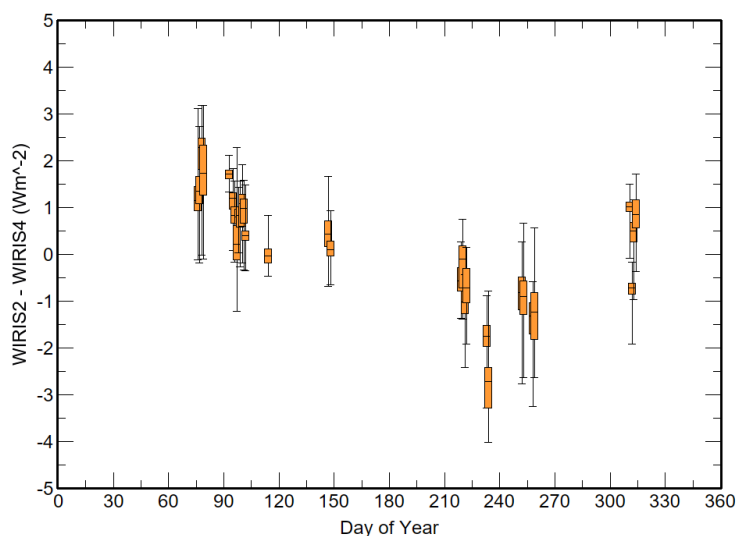
During 2020 data from ACP96 were recorded at PMOD/WRC sometimes coincidentally with IRIS4 and IRIS2. Night-time data were available from ACP96 and IRIS2 between 7 January 2020 and 10 December 2020, and between 15 March and 10 December for IRIS4. The data consisted of an average value every 60 seconds for any IRIS irradiance and for ACP96 a 1 s measurement sequence every 10 seconds. Simultaneous measurements were available for 41 days with IRIS2 and 36 days with IRIS4.

Figure 1 shows a Box-Whisker representation of the differences between the simultaneous measurements of atmospheric terrestrial irradiances  $W_{IRIS2}$  and  $W_{IRIS4}$ . The typical daily range in differences is  $1.5 \text{ Wm}^{-2}$  which is within the individual



instrument expanded ( $k=2$ ) of  $2 \text{ Wm}^{-2}$  (Gröbner, 2012). Slightly larger differences, with IRIS2 lower than IRIS4, are observed on two days in August (day of year 233 and 234), which are still within the combined uncertainties of the two radiometers. There appears to be a trend in the daily mean differences until day 260 and then a restoration of the early 2020 mean daily differences after day 300.

While there appears to be a drift between the two data sets it was decided to use both data sets as a reference or comparison data set. These IRIS data tested the impact of using different reference irradiances and were used to corroborate the results of the methods described below.



290 **Figure 1. Statistics for the difference between  $W_{IRIS2}$  and  $W_{IRIS4}$  for every simultaneous irradiance in 2020 in Box-Whisker plots.**

## 8.2 Deriving $K_I$ or $C$ from an estimated solar calibration of the thermopile

For this method either prior to an ACP being assembled or by removing ACP's concentrator, the concentrator is replaced with a pyrheliometer aperture system that conforms to pyrheliometer requirements, with the closest aperture to the receiver surface being identical to the aperture of the concentrator. It would be pointed at the Sun and compared to a well calibrated WRR (or SI) pyrheliometer to produce an estimate of the thermopile responsivity to solar irradiance. That estimate would then be converted to the infrared responsivity by assuming the emissivity of the receiver surface for both solar ( $\epsilon_{solar}$ ) and infrared emission ( $\epsilon$ ).

Unfortunately, no solar calibration exists for the thermopile of ACP96 so an estimate had to be made.



300 The absorptivity of a F3 thermopile receiver used for solar measurements in a PSP pyranometer and terrestrial infrared by the PIR pyrgeometer is known to decrease with time due to long term exposure dependent on integrated total solar exposure ( $\text{Jm}^{-2}$ ), but a F3 thermopile used in a PIR decays slowly as it is not subjected to solar exposure. As a PIR requires monitoring of the temperature of the base of the thermopile, it is ideally suited to conversion to an ACP and its thermopile receiver surface has not been subjected to high levels of solar exposure. One we will assume an ACP thermopile responsivity for solar irradiance  $C_s$  would likely be that of a new F3 thermopile.

305 The calibrations of new PSP pyranometers were then used to estimate a likely solar calibration for a F3 in an ACP. The data from over 82 individual PSP calibrations sourced from Eppley Laboratory and multiple national calibration centres in the USA, Canada and Australia indicated that the mode and mean solar sensitivities of new PSPs manufactured after 2000 was  $\sim 9.3 \mu\text{V}/(\text{Wm}^{-2})$ .

If  $C_{solar}$  is the derived responsivity using the Sun for infrared measurements with an ACP F3 thermopile,

310 
$$C = \frac{\epsilon_r C_{solar}}{\tau_{dome}^2 \epsilon_{rsolar}} \quad (24)$$

As Parsons Black is used to coat the receiver surface, with a typical receiver solar emissivity  $\epsilon_{rsolar} \sim 0.98$  and for infrared  $\epsilon_r \sim 0.92$ , and a PSP has a double dome with both domes having a nominal transmission at solar wavelengths of  $\tau_{dome} \sim 0.91$ , then this gives an estimate of  $C \sim 10.5 \mu\text{V}/(\text{Wm}^{-2})$ .

315 Using the new equation, the atmospheric irradiance  $W_{ACP96}$  was calculated when both IRIS4 and IRIS2 were operating and ACP96 was monitoring in steady state night-time conditions. This resulted in comparisons over 41 nights (18802 measurements) with IRIS2 and 33 nights (14085 measurements) with IRIS4. The results are presented in Table 1 using  $C=10.5$ ,  $\gamma=8.4$ ,  $\tau=0.977$  and  $\epsilon_s=0.0225$ ; the daily mean differences ( $W_{IRIS2} - W_{ACP96}$ ) and ( $W_{IRIS4} - W_{ACP96}$ ) for each of the days are shown in Figure 2. A second set of statistics are presented in Table 2 and figure 3 using  $\gamma=6.5$ .

320 **Table 1. The mean differences and the statistics of ( $W_{IRIS2} - W_{ACP96}$ ) and ( $W_{IRIS4} - W_{ACP96}$ ) in  $\text{Wm}^{-2}$  for data from January to November 2020, using  $C=10.5$ ,  $\gamma=8.4$ ,  $\tau=0.977$  and  $\epsilon_s=0.0225$ .**

	Number	Average	Std Deviation	Maximum	Minimum
$W_{IRIS2} - W_{ACP96}$	18802	0.23	1.21	2.64	-3.70
$W_{IRIS4} - W_{ACP96}$	14085	-0.18	0.88	2.03	-2.54

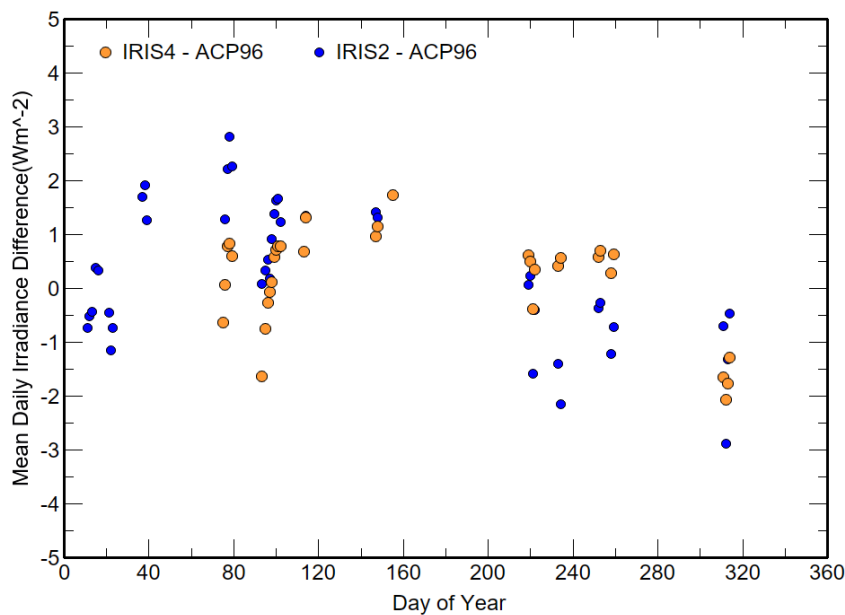
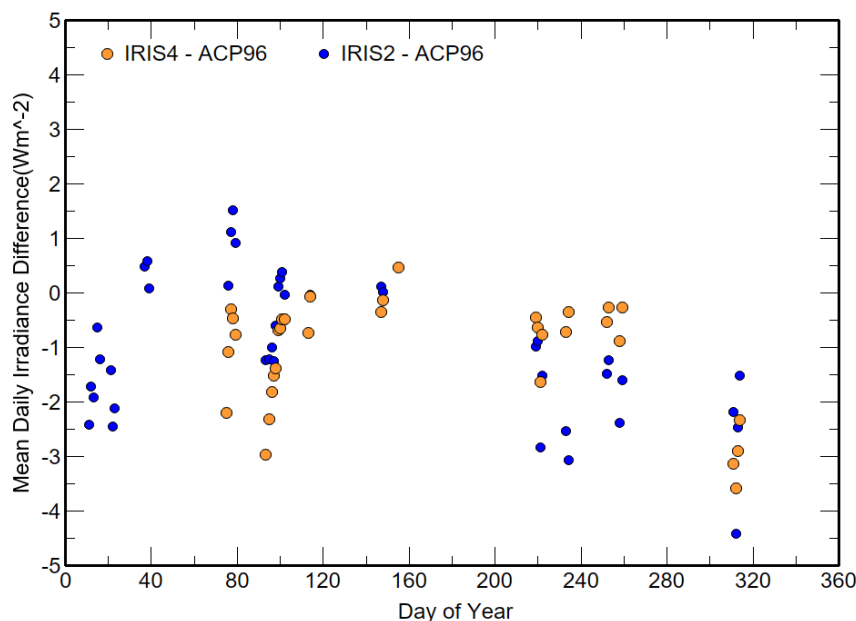


**Figure 2.** The daily mean differences and the statistics of  $(W_{IRIS2} - W_{ACP96})$  and  $(W_{IRIS4} - W_{ACP96})$  in  $Wm^{-2}$  from January to November 2020, using  $C=10.5$ ,  $\gamma=8.4$ ,  $\tau=0.977$  and  $\varepsilon_c=0.0225$ .

325 **Table 2.** The mean differences and the statistics of  $(W_{IRIS2} - W_{ACP96})$  and  $(W_{IRIS4} - W_{ACP96})$  in  $Wm^{-2}$  for data from January to November 2020, using  $C=10.5$ ,  $\gamma=6.5$ ,  $\tau=0.977$  and  $\varepsilon_c=0.0225$ .

	No	Mean	Std Deviation	Maximum	Minimum
$W_{IRIS2} - W_{ACP96}$	18802	-1.07	1.44	2.54	-5.55
$W_{IRIS4} - W_{ACP96}$	14085	-1.26	1.08	1.14	-4.71



330 **Figure 3.** The daily mean differences and the statistics of  $(W_{IRIS2} - W_{ACP96})$  and  $(W_{IRIS4} - W_{ACP96})$  in  $\text{Wm}^{-2}$  from January to November 2020, using  $\gamma=6.5$  and  $C=10.5$ ,  $\tau=0.977$ ,  $\epsilon_c=0.0225$ .

The differences to  $W_{IRIS2}$  were larger than for  $W_{IRIS4}$ , and there appears to be a similar trend in the relationship between IRIS2 and ACP96, as seen with the comparison between  $W_{IRIS2}$  and  $W_{IRIS4}$ . The differences between Table 1 and Table 2 shows the impact of a 22% change in  $\gamma$  for steady state conditions is  $0.6 \text{ Wm}^{-2}$  APC96 irradiance difference for a  $\Delta\gamma = 1$ . Decreasing  $\gamma$  by -1.9 shifted all the mean values down by  $\sim 1.2 \text{ Wm}^{-2}$  but increased the range of the  $W_{IRIS2}-W_{ACP96}$  while the  $W_{IRIS4}-W_{ACP96}$  showed little change.

335

### 8.3 Field calibration using a reference irradiance

This method also assumes fixed values for the concentrator emissivity  $\epsilon_c$ , and convection coefficient  $\gamma$  and finds the minimum difference between the reference irradiance  $W_{IRIS2}$  or  $W_{IRIS4}$ , and  $W_{ACP96}$  using paired values of  $K_1$  and concentrator transmission  $\tau$ . That is, for a set of  $n$  observations made up of  $m$  nights ideally with ranges in  $W_{IRIS}$  and  $W_{ACP96}$ , the pair  $[C, \tau]$  is found that provides a mean difference of  $(W_{IRIS} - W_{ACP96})$  of less than  $0.1 \text{ Wm}^{-2}$ . Given the low irradiance impact of concentrator emissivity, and convection coefficient in steady state conditions, the convergence to a solution is straight forward.

340

In the  $\gamma=8.4$  set the  $(W_{IRIS}-W_{ACP96})$  statistics for simultaneous measurements with IRIS2 and IRIS4 observations are presented in Table 3. There are differences of 0.4 (or  $\sim 4\%$ ) between the  $C$  values and 0.011 ( $\sim 1.2\%$ ) between the resultant concentrator



transmission values. The table also presents the results of using the average of the two  $C$  and transmission values derived from  
 345 IRIS2 and IRIS4 giving  $C=10.5$  and  $\tau=0.9764$  and deriving the difference statistics to both IRIS2 and IRIS4.

**Table 3.** The statistics of  $W_{IRIS}-W_{ACP96}$  using  $\epsilon_c=0.0225$  and  $\gamma=8.4$  from March to November 2020, for the pairs of  $C$  and  $\tau$  that minimize the mean difference of  $W_{IRIS}-W_{ACP96}$ . The difference statistics using the average  $C$  and  $\tau$  of the IRIS2 and IRIS4 results are also given in the last two rows of the table.

	$No$	$ACP96$ $C$	$ACP96$ $\tau$	$W_{IRIS}-$ $W_{ACP96}$ Average	$W_{IRIS}-$ $W_{ACP96}$ Std Dev	$W_{IRIS}-$ $W_{ACP96}$ Max	$W_{IRIS}-$ $W_{ACP96}$ Min
$W_{IRIS2}-W_{ACP96}$	18802	10.72	0.9820	0.04	1.08	3.90	-4.24
$W_{IRIS4}-W_{ACP96}$	14085	10.28	0.9707	-0.03	0.96	2.30	-3.37
$W_{IRIS2}-W_{ACP96}$	18802	10.50	0.9764	-1.19	1.44	2.42	-5.68
$W_{IRIS4}-W_{ACP96}$	14085	10.50	0.9764	-1.39	1.07	1.00	-4.84

350 If the three  $C$  values in Table 3 are converted to equivalent PSP F3 thermopile solar  $C$  values it results in values centred on 9.35 +/- 0.3, all within 3.5%.

The process was repeated but using a convection coefficient  $\gamma$  of 6.5, with the results are presented in Table 4. The standard deviations and range of differences increase slightly when compared to the values derived using 8.4 for the convection coefficient. The resultant  $C$  values were reduced by 0.2, while the transmission values are reduced by ~0.0013. However,  
 355 unlike the results in Table 3, the average differences were much smaller in magnitude.

**Table 4.** The statistics of  $(W_{IRIS}-W_{ACP96})$  using  $\epsilon_c=0.0225$  and  $\gamma=6.5$  from March to November 2020, for pairs of  $C$  and  $\tau$  found that minimize the standard deviation of the  $(W_{IRIS}-W_{ACP96})$ . The difference statistics using the average  $C$  and  $\tau$  of the IRIS2 and IRIS4 results are also given in the last two rows of the table.

	$No$	$ACP96$ $C$	$ACP96$ $\tau$	$W_{IRIS}-$ $W_{ACP96}$ Average	$W_{IRIS}-$ $W_{ACP96}$ Std Dev	$W_{IRIS}-$ $W_{ACP96}$ Max	$W_{IRIS}-$ $W_{ACP96}$ Min
$W_{IRIS2}-W_{ACP96}$	18802	10.51	0.9819	0.08	1.41	3.67	-4.39
$W_{IRIS4}-W_{ACP96}$	14085	10.06	0.9692	-0.04	0.99	2.23	-3.28
$W_{IRIS2}-W_{ACP96}$	18802	10.28	0.9756	0.19	1.43	3.71	-4.06



$W_{IRIS4}-W_{ACP96}$	14085	10.28	0.9756	-0.03	1.04	2.32	-3.38
-----------------------	-------	-------	--------	-------	------	------	-------

360 The results in Tables 3 and 4 indicate that a negative 22% change in the convection coefficient reduces  $C$  by 2% and increases the transmission by 0.1% to achieve mean irradiance differences less than  $0.1 \text{ Wm}^{-2}$ . These changes are self-consistent given the high correlation between the components of the ACP equations either of Reda et al., 2012 or the new equation and shows a  $2 \text{ Wm}^{-2}$  impact with a change in the convection component of 1.9. However, for the averaged values of  $C$  and transmission the lower convection coefficient provided the averages closest to zero for both reference irradiance. The transmissions in Table  
 365 3 and 4 from using the mean of the IRIS2 and IRIS4 results are within 0.002 of the 0.977 value derived for ACP95 using the new equation and NIST laboratory measurements.

The small differences ( $W_{IRIS2}-W_{IRIS4}$ ) for two days in August and the high correlation between components in the new equation demonstrates that uncertainty in the reference irradiance impacts the minimization method and shows the benefit of having multiple reference irradiances to assess confidence intervals.

370 The increase in  $C$  with an increase in transmission and the magnitude of these changes is a consequence of the difference in the measured  $W_{IRIS2}$  and  $W_{IRIS4}$ . Of the 4 components of  $W_{atm}$  in the new equation two dominate, namely the thermopile voltage and the thermopile blackbody irradiance  $W_r$ ; the contributions from  $W_c$  and  $(T_r - T_c)$  are less than 4%. The magnitude of the irradiance derived from the thermopile signal is of the order of  $-80 \text{ Wm}^{-2}$  while for  $W_r$  is typically between 300 and  $500 \text{ Wm}^{-2}$ . Hence if the minimization method is to achieve a balance between  $K_1$  and transmission, for a  $1 \text{ Wm}^{-2}$  change in reference  
 375 irradiance, then  $K_1$  changes by the higher percentage as the  $W_r$  is unchanged. If only  $K_1$  was minimized instead of a  $(K_1, \tau)$  pair, then a  $\Delta \text{ Wm}^{-2}$  difference if  $W_{atm}$  would result in  $K_1$  changing by  $\Delta/W_r$ . Further complications arise if the relationship between the true  $W_{atm}$  and  $W_{ref}$  changes.

#### 8.4 Adaption of Reda et al., 2012 linear LSQ calibration method to the new equation

380 From Eq. (18) and assuming the fraction of backscatter of incoming irradiance  $\beta$  is zero we can define the predictand for the linear LSQ analysis as

$$y(W_r, W_c, T_r, T_c, t) = W_{net}(t) = W_r(t) - \varepsilon_c W_c(t) + \gamma(T_r(t) - T_c(t)) \quad (25)$$

with the thermopile voltage  $V$  the predictor for the linear LSQ analysis, hence the equation to solve by linear LSQ is

$$y(W_r, W_c, T_r, T_c, t) = W_{net}(t) = \langle K_1 \rangle V(t) + \langle \tau W_{atm} \rangle \quad (26)$$

385 which results in a  $\langle C \rangle = 1 / \langle K_1 \rangle$  and is independent of concentrator transmission. From  $\langle \tau W_{atm} \rangle$  by assuming a value for the concentrator transmission results in values for  $\langle W_{atm} \rangle$  which could be compared to a reference irradiance or its inverse by prescribing a reference irradiance and derive a concentrator transmission.





For the linear LSQ process to be successful,  $W_{atm}$  and  $\gamma$  must be constant during the data collection process and the ACP equation must be valid. In stable  $W_{atm}$  conditions, the process for collecting the required rapid cooling periods results in only small changes in  $T_c$  and  $W_c$ . As a result, the changes in concentrator irradiance component  $\varepsilon_c W_c$  are less than  $0.1 \text{ Wm}^{-2}$  over the entire rapid cooling process, and hence minimal impact on  $\langle K_1 \rangle$ .

Given the properties of linear LSQ, using a single predictor,  $V(t)$ , if the predictand is made up of multiple linear components one can solve for each component of the predictands independently. The three predictand components from Eq. (18) are

$$W_r(t) = y_r(t) = \langle A_r \rangle V(t) + \langle B_r \rangle \quad (27)$$

Similarly

$$W_c(t) = y_c(t) = \langle A_c \rangle V(t) + \langle B_c \rangle \quad (28)$$

and lastly

$$dT(t) = (T_r(t) - T_c(t)) = y_{dT}(t) = \langle A_{dT} \rangle V(t) + \langle B_{dT} \rangle \quad (29)$$

$dT(t)$  can also be split into three separate components, but that will be left to the discussion section of this paper on the impact of incorrect estimates of the Seebeck coefficient and assuming  $T_c(t)$  is equivalent to  $T_{air}(t)$ .

Derived  $\langle K_1 \rangle$  and  $\langle \tau W_{atm} \rangle$  using the new equation are given by

$$\langle K_1 \rangle = \langle \frac{1}{c} \rangle = \varepsilon_c \langle A_c \rangle - \langle A_r \rangle - \gamma \langle A_{dT} \rangle \quad (30)$$

and

$$\langle \tau W_{atm} \rangle = \langle B_r \rangle - \varepsilon_c \langle B_c \rangle + \gamma \langle B_{dT} \rangle \quad (31)$$

Given  $W_c$  is almost constant through the  $\sim 7$  minute cooling of the thermopile, and  $|\langle A_c \rangle| < 0.005$ , then  $|\varepsilon_c \langle A_c \rangle| < 0.00015$  and contributes less than 0.1% to  $\langle K_1 \rangle$ , hence the concentrator emissivity has minimal impact on deriving  $\langle K_1 \rangle$  using the new equation. For the intercept terms  $\varepsilon_c \langle B_c \rangle$  typically makes a small negative contribution to  $\langle \tau W_{atm} \rangle$  of the order of 2.5%.  $W_r$  and  $(T_r - T_c)$  dominate contributions to both  $\langle K_1 \rangle$  and  $\langle \tau W_{atm} \rangle$ .

The concentrator transmission is irrelevant to deriving  $\langle \tau W_{atm} \rangle$  or  $\langle K_1 \rangle$  but is essential to estimating  $\langle W_{atm} \rangle$  from  $\langle \tau W_{atm} \rangle$ . If  $W_{atm}$  is known through a reference radiometer ( $W_{ref}$ ), then the concentrator transmission can be estimated by

$$\tau = \frac{\langle \tau W_{atm} \rangle}{W_{ref}} \quad (32)$$

For any linear LSQ process there is a key requirement that the process is linear, and in this specific case  $\tau W_{atm}$  must be constant. As a result, initial criteria for acceptable conditions were established for a valid linear LSQ analysis period.

When the base of the ACP is cooled rapidly, the thermopile signal must continuously become less negative. As the thermopile voltage was measured every 10 seconds, the start point of a linear LSQ was defined as when the difference in consecutive



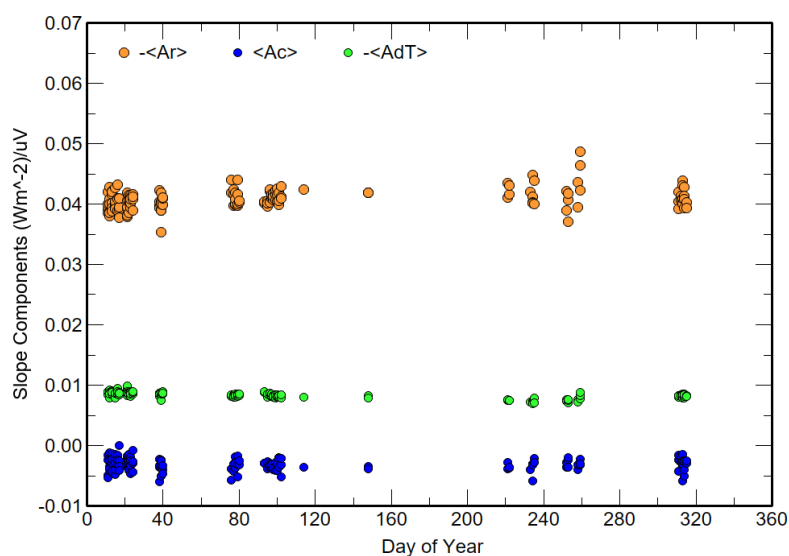
415 thermopile voltages was more than  $+3.5 \mu\text{V}$  and the linear LSQ sequence was deemed to stop if the voltage difference between two consecutive voltage was least than or equal to  $+3.5 \mu\text{V}$ . Similarly, the start of a linear LSQ also required the difference in consecutive  $(T_r(t)-T_c(t))$  to be less than  $-0.04 \text{ K}$  and a linear LSQ sequence was also deemed to stop if the temperature decrease was greater than or equal to  $-0.04 \text{ K}$ . The next criterion involved the total voltage increase over a cooling sequence: if the total range of the voltage was less than  $200 \mu\text{V}$  the period was rejected. The last criterion required

420  $(T_r-T_c)(t_i)-(T_r-T_c)(t_{i-1}) < 0.02$

this ensured that cooling was not nearing the new base temperature or that the cooling process was being reversed.

Out of 266 possible periods during 2020 for ACP96, 244 linear LSQ calibration periods satisfied the criterion. Figures 4 and 5 show the time series of the individual slopes  $\langle A_c \rangle$ ,  $\langle A_r \rangle$ ,  $\langle A_{dT} \rangle$ , and intercepts  $\langle B_r \rangle$ ,  $\langle B_c \rangle$ ,  $\langle B_{dT} \rangle$  derived from the valid linear LSQ analyses.  $\langle A_c \rangle$ ,  $\langle A_r \rangle$  are stable about a mean value but the slopes for  $(T_r-T_c)$ , and  $\langle A_{dT} \rangle$ , shows an upwards shift

425 between days 200 and 255 that recovers when data collection recommenced on day 312; meteorological data for these periods indicates the dew point temperature was less than  $4 \text{ K}$  below the ambient temperature and thermopile surface temperatures during cooling were close to or less than the dew point. While  $\langle B_{dT} \rangle$  is relatively constant over the year, as expected  $\langle B_r \rangle$  and  $\langle B_c \rangle$  follow the irradiance of the ambient temperature peaking in summer periods.



430 **Figure 4.** The linear LSQ slope  $\langle A_r \rangle$ ,  $\langle A_c \rangle$  and  $\langle A_{dT} \rangle$  components that generate  $\langle K_1 \rangle$  for 244 calibrations in 2020.

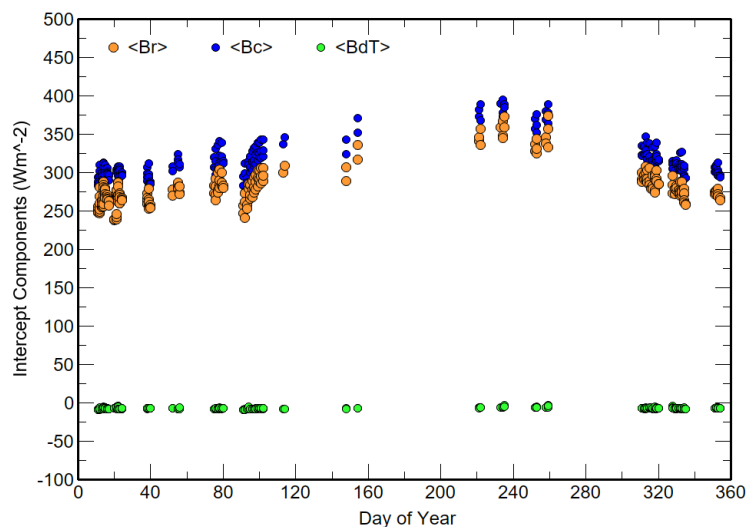
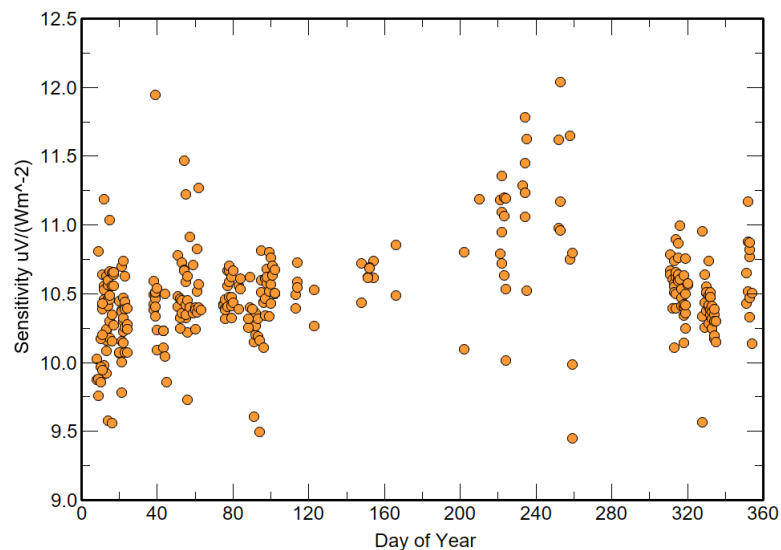


Figure 5. The linear LSQ slope  $\langle B_r \rangle$ ,  $\langle B_c \rangle$  and  $\langle B_{dT} \rangle$  components that generate  $\langle \tau W_{atm} \rangle$  for 244 calibrations in 2020.

The thermopile responsivities  $\langle C \rangle$  found for 244 linear LSQ calibration periods are shown in Figure 6.



435 Figure 6. ACP96  $\langle C \rangle$  values derived using the new equation using the linear LSQ method with  $\epsilon_c = 0.0225$ ,  $\gamma = 6.5$  for 244 calibration periods in 2020.



There were 115 periods that were coincident with IRIS2 measurements when the standard deviation of  $W_{IRIS2}$  in a cooling sequence was less than  $0.4 \text{ Wm}^{-2}$  and 63 coincident with IRIS4 also with a standard deviation less than  $0.4 \text{ Wm}^{-2}$ .  $\langle C \rangle$  statistics for the 244 linear calibration periods and irradiance differences for the coincident periods with  $W_{IRIS2}$  or  $W_{IRIS4}$  are presented in Tables 5 and 6 for  $\gamma=6.5$  and  $\gamma=8.4$  respectively.

**Table 5. Linear LSQ method results for ACP96  $\langle C \rangle$  and  $W_{IRIS2} - \langle W_{atm} \rangle$  calculations used  $\varepsilon_c = 0.0225$ ,  $\gamma=6.5$  and  $\tau=0.977$  for the total 244 linear LSQ calibrations regardless of the stability of  $W_{atm}$  and 115 periods in 2020 when IRIS2 data and 63 periods when IRIS4 data were available, and the standard deviation of  $W_{atm}$  from an IRIS was less than  $0.4 \text{ Wm}^{-2}$ .**

Parameter	Mean	N	$\sigma$	Max	Min
$\langle C \rangle$	10.49	244	0.36	12.04	9.45
$\sigma_{IRIS2} < 0.4 \text{ Wm}^{-2}$					
$\langle C \rangle$	10.47	115	0.25	11.42	9.98
$W_{IRIS2} - \langle W_{ACP} \rangle$	-0.04	115	2.23	3.98	-6.85
$\sigma_{IRIS4} < 0.4 \text{ Wm}^{-2}$					
$\langle C \rangle$	10.58	63	0.26	11.42	10.01
$W_{IRIS4} - \langle W_{ACP} \rangle$	-1.19	63	1.80	2.76	-5.83
$W_{IRIS2} - W_{IRIS4}$	0.69	63	1.12	2.94	-1.30

**Table 6. Linear LSQ method results for ACP96  $\langle C \rangle$  and  $W_{IRIS2} - \langle W_{atm} \rangle$  calculations used  $\varepsilon_c = 0.0225$ ,  $\gamma=8.4$  and  $\tau=0.977$  for 115 periods in 2020 when IRIS2 data and 63 periods when IRIS4 data were available, and their period standard deviation was less than  $0.4 \text{ Wm}^{-2}$ .**

Parameter	Mean	N	$\sigma$	Max	Min
$\sigma_{IRIS2} < 0.4 \text{ Wm}^{-2}$					
$\langle C \rangle$	8.58	115	0.26	9.75	7.90
$W_{IRIS2} - \langle W_{ACP} \rangle$	13.16	115	3.20	17.92	2.16
$\sigma_{IRIS4} < 0.4 \text{ Wm}^{-2}$					
$\langle C \rangle$	8.70	63	0.28	9.75	8.21



$W_{IRIS4} - \langle W_{ACP} \rangle$	11.68	63	2.95	17.28	2.47
---------------------------------------	-------	----	------	-------	------

The differences ( $W_{IRIS2} - \langle W_{atm} \rangle$ ) and ( $W_{IRIS4} - \langle W_{atm} \rangle$ ) for coincident measurements are shown in Figure 7 with the convection coefficient used value is 6.5. The results between days 200 and 254 for both  $\langle C \rangle$  and the  $\langle W_{atm} \rangle$  appear anomalous with significantly higher values of  $\langle C \rangle$  and underestimates of the irradiance differences; these are during periods when the steady state base temperature is typically high for the year and within 4 K of the dew point temperature and high relative humidity. The periods before day 200 and after day 300 give consistent  $\langle C \rangle$  values about a mean as did the irradiance differences. The means of pre day 200 and post day 300 are separated by about  $2.2 \text{ Wm}^{-2}$ . Given that  $\langle C \rangle$  is likely constant over the two periods it suggests that either the reference IRIS irradiances calibration may have changed, or the transmission of the concentrator may have decreased.

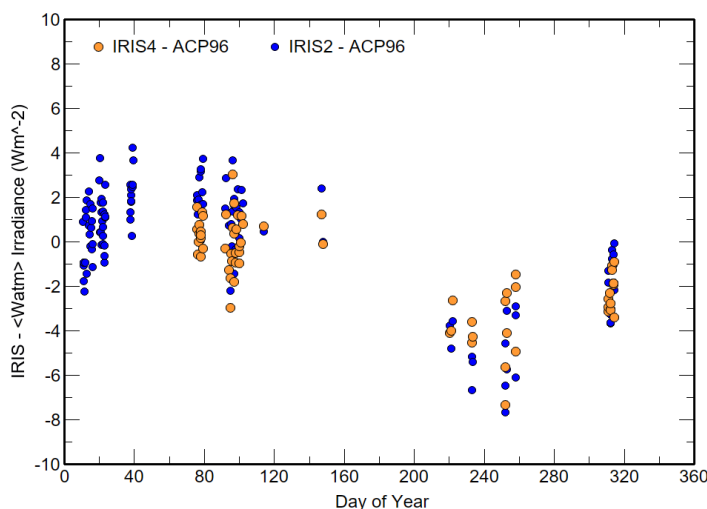


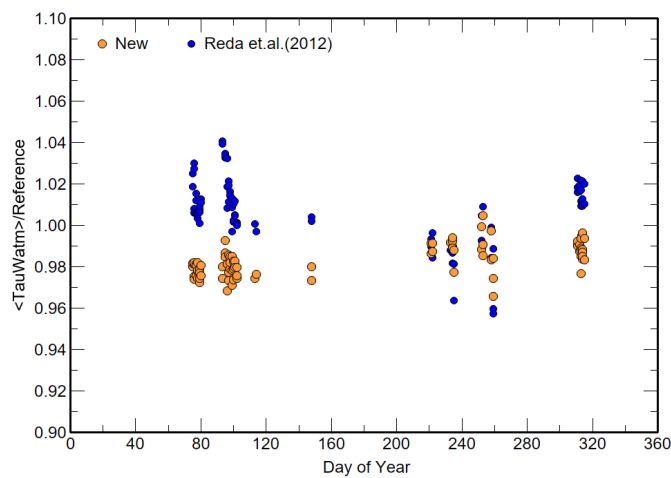
**Figure 7.** Daily mean irradiance differences ( $W_{IRIS} - \langle W_{atm} \rangle$ ) between the mean IRIS ( $W_{IRIS}$ ) and linear LSQ interpolated ACP96 ( $\langle W_{atm} \rangle$ ), using the new equation with  $\epsilon_c = 0.0225$ ,  $\gamma = 6.5$ , and  $\tau = 0.977$ .

The mean derived  $C$  value in Table 5 using 6.5 as the convection coefficient is  $10.49 \mu\text{V}/(\text{Wm}^{-2})$  which is within  $0.3 \mu\text{V}/(\text{Wm}^{-2})$  of the solar and minimization methods. Table 6 using the higher convection coefficient of 8.4 shows a mean  $C$  about 18% lower and the irradiance differences greater than  $11 \text{ Wm}^{-2}$  between the ACP96 and IRIS2 and IRIS4.

No attempt was made to adjust the concentrator transmission  $\tau$  based on the derived  $C$  (or  $K_1$ ), as it is a property of the concentrator not the thermopile. However, it was possible to estimate  $\tau$  using the derived  $\langle \tau W_{atm} \rangle$  from the linear LSQ intercept which is independent of any assumed value of  $\tau$  by dividing  $\langle \tau W_{atm} \rangle$  by  $W_{IRIS4}$ ; similarly, the derived  $\langle \tau W_{atm} \rangle$  from the Reda et al., 2012 equation could also produce an estimate of the concentrator transmission  $\tau$ . Figure 8 shows the results of dividing



the  $\langle \tau W_{atm} \rangle$  derived from both LSQ equations by IRIS4 data. Similar results were obtained using  $W_{IRIS2}$ . The results using the new equation suggest a concentrator transmission  $\tau \sim 0.98$ , while for the Reda et al., 2012 equation a significant majority of periods gave unphysical values of  $\tau$  greater than 1.



470

**Figure 8.** Concentrator transmission estimates derived from dividing the linear LSQ obtained  $\langle \tau W_{atm} \rangle$  by  $W_{IRIS4}$  for 63 estimates using the new equation (18) and the Reda et. al. (2012) equation (22) estimate of  $\langle \tau W_{atm} \rangle$ .

### 8.5 Ensuring the representativeness of $\tau W_{atm}$ during a linear LSQ calibration period

The thermopile voltage measurement is a consequence of net irradiance based on the temperature difference of the base of the thermopile to the top of the thermopile. The black body equivalent irradiance of the thermopile receiver is calculated by assuming the Seebeck coefficient is valid and the body temperature represents the temperature at the base of the thermopile. Provided the time constants of the thermopile and thermistors are similar and the heating or cooling of the body are not too rapid, the  $C$  and convection coefficient should provide  $\tau W_{atm}$  for all measurements (or  $K_1$  Eq. (22)) and ideally produce a near constant value during both cooling and heating.

Using the data for ACP96 in 2020, and the calculated mean values of  $C$  given in Table 5, the individual cooling and heating periods were examined and found to maintain some repeatable oscillations that could not be eliminated by changing either the convection coefficient or  $C$  for the new equation; for the Reda et al., 2012 equation only  $K_1$  could be varied and resulted in decreases of calculated irradiances over the cooling and heating period regardless of the  $K_1$  used.

The sinusoid shape of the oscillation in the derived  $\tau W_{atm}$ , higher during cooling and lower during heating, suggested that there was a phase difference between the thermopile voltage and the body temperature or some processes unaccounted for using the new equation. If a phase issue, the thermopile voltage at measurement period  $p$  was lagging the changing body temperature,

485



and hence the temperature of the body at time  $t$  was not representing the temperature of the thermopile base at  $t$ . Such differences would be tiny in steady state conditions given the slow rate of change in  $T_b$ .

490 Linear interpolation in time was used to find a more representative thermopile voltage that removed the sinusoidal oscillation in  $\tau W_{atm}$ . It was found that for ACP96 a lag time of about  $9\text{ s} \pm 2\text{ s}$  was required to remove the majority of oscillations for the new equation; it also reduced the magnitude of the depression from true irradiance using the Reda et al., 2012 equation. Given measurements for all quantities were repeated every 10 s, the most representative thermopile voltage for measurement  $p$  every 10 s,  $V_{p'}$  was

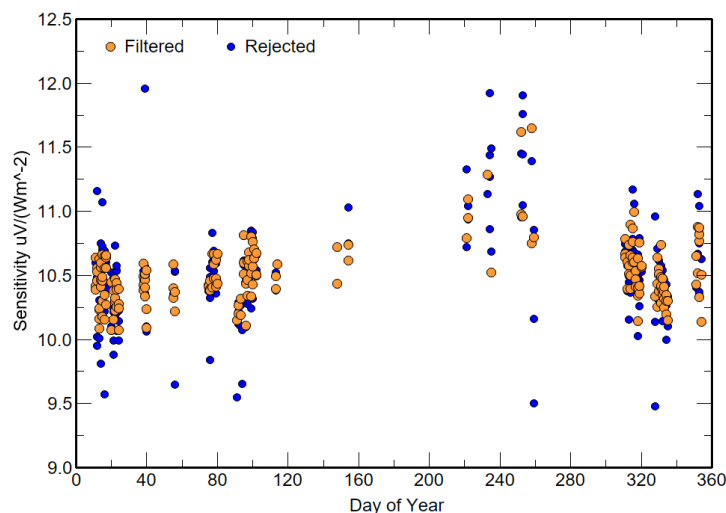
$$V_{p'} = V_p + 0.9 (V_{p+1} - V_p) \quad (33)$$

495 Using this interpolated voltage  $V_{p'}$  to represent the thermopile voltage at  $p$ , resulted in significantly improved standard errors and confidence intervals for each of the linear LSQ derived components of  $\langle K_1 \rangle$  and  $\langle C \rangle$  by factors of 3 to 10 depending on the linear LSQ component and provided statistics for the variation of  $\tau W_{atm}$  throughout each cooling and heating period. The improved linear LSQ fits did not impact significantly on the derived  $\langle K_1 \rangle$  or  $\langle C \rangle$  only raising  $\langle C \rangle$  by less than 0.02, with no significant difference to the results presented in section 8.4.

500 The phase shift showed that both the new and Reda et.al., 2012 equations could represent the changing incoming irradiance through the cooling and heating with varying degrees of success. It also provided a cumbersome visual method to derive  $C$  and the convection coefficient by minimizing the variation of  $\tau W_{atm}(t)$  during the cooling and heating cycles.

Most importantly, it provided a method of judging if  $\tau W_{atm}$  was nominally constant during a linear LSQ calibration period and thus removed the requirement of a reference radiometer for that purpose.

505 Using equation (33) to represent the thermopile signal for measurement  $p$ , and setting a standard deviation of  $\tau W_{atm}$  over the cooling and heating period was below  $0.6\text{ Wm}^{-2}$  was acceptable, the results for  $\langle C \rangle$  derived by linear LSQ in section 8.4 were re-examined. Figure 9 shows the same  $\langle C \rangle$  values as in Figure 7 and those that satisfy the standard deviation of  $\tau W_{atm}$  criterion. Of the 244 original values, only 51 were removed because of the larger standard deviation in  $\tau W_{atm}$  over the cooling period. The main impact was removal of outliers. It had little impact on the divergence of results between days 200 and 260 in 2020.



510

**Figure 9.** Responsivity  $\langle C \rangle$  values presented in figure 7 but filtered for standard deviations of ACP96  $\tau W_{atm}$  during the cooling period that are less than  $0.6 \text{ Wm}^{-2}$  are gold, and those with higher standard deviations are in blue.

## 9 Discussion

The four different methods using the new ACP irradiance equation to calibrate the ACP96 provided irradiances compared well with the irradiances from IRIS2 and IRIS4 during 2020. One was based on laboratory or blackbody estimates for concentrator emissivity and transmission and the convection coefficient an estimate of  $C$  based on the modal value over 80 new F3 thermopile solar calibrations. Another used minimization of the differences between the ACP and IRIS radiometers for pairs of  $C$  and concentrator transmission. The third was use of the same methodology of Reda et al., 2012 but using the new equation. The fourth used the derived calibrations in third method to estimate  $\tau W_{atm}$  from every measurement during a cooling and heating period and thereby filter the results for stable periods without the need for a separate pyrgeometer. All methods produced mean differences from IRIS2 and IRIS4 less than  $1.2 \text{ Wm}^{-2}$  and typically ranges of  $\pm 3 \text{ Wm}^{-2}$  from the mean difference for IRIS4. The differences in irradiances between IRIS2 and ACP96 were not symmetric about the mean, suggesting an identical trend in calibration of either both ACP96 and IRIS4 simultaneously or just IRIS2. As the year progressed the daily mean differences between IRIS2 and ACP96 became increasingly negative until day 300 when irradiances recovered and equated to IRIS4 as during March and April 2020.

That the pseudo solar calibration method produced a value very close to the other methods was fortuitous given that it was based on the modal value of initial PSP calibrations based on  $\sim 80$  instruments. The range of potential values matched the derived results and suggests that a solar calibration of the ACP F3 thermopile is both a useful first step in characterising an





530 ACP thermopile as well as estimating the maximum potential ACP IR calibration and the method could be used periodically  
to check the stability of the thermopile. An extended solar calibration over ambient temperature ranges using the method of  
Pascoe and Forgan (1980) could also confirm the temperature compensation of the thermopile. However, given the decadal  
decrease in responsivity of the F3 thermopiles in PSP radiometers, exposure of an ACP thermopile to solar exposure should  
be kept to a minimum to reduce the impact of solarization of the Parsons Black paint. Using the solar method as a primary  
calibration also negates the ACP as an absolute irradiance reference standard as well as being based on likely historical  
535 estimates of the expected emissivity of Parsons Black in both the IR and solar wavelengths. However, as most World  
Meteorological Organization regional instrument centres have ready access to well-maintained reference pyrhemometers but  
not laboratory facilities to characterize the concentrator it could with further work, prove useful verification and monitoring  
tool.

At a minimum, the solar calibration will provide a lower limit for  $K_1$  (and hence an upper limit for  $C$ ). That the theoretical  
540 value derived from the nominal solar calibration from an ensemble of new PSP F3 thermopiles gave mean deviations of less  
than  $1.5 \text{ Wm}^{-2}$  for over 14000 measurements with a standard deviation of  $\sim 1 \text{ Wm}^{-2}$  supports this recommendation.

The second method used an IR reference irradiance to solve for both  $C$  and concentrator transmission simultaneously. The  
reference pyrgeometers, both IRIS, are not influenced by calibration coefficients dependent on the spectral transmission and  
emission of IR of the domes. However, it was clear from the 2020 comparison data that any reference radiometer must have  
545 an up-to-date calibration, with distinct steps and trends in the derived relationship between the ACP and IRIS radiometers in  
the comparison data. However, irradiance differences are all well within the current WMO traceability requirement for  
terrestrial irradiances of  $5 \text{ Wm}^{-2}$ .

The concentrator transmission derived for ACP95 using the data from Jinan et. al. (2010) but the new equation, and the NIST  
value of concentrator emissivity reported by Reda et al., 2012, were applied to ACP96 and produced good agreement with the  
550 IRIS2 and IRIS4 measurements regardless of the methods described above. This suggests that these parameters could be used  
as a first approximation for any ACP. However, if an ACP is to be used without reference to a blackbody or reference  
radiometer, the concentrator emissivity should be obtained independently in the laboratory using the laboratory techniques  
reported by Reda et al., 2012 and the impact of a significant error in the emissivity for any irradiance calculation by the new  
equation would be small. As the difference between the true versus assumed concentrator transmission  $\tau$  would have a directly  
555 proportional effect on  $W_{atm}$ , an alternative method to obtain the concentrator emissivity would be to repeat the Jinan et al.,  
2010 methodology for each ACP but using the new equation to generate a concentrator transmission and then assume the  
emissivity is  $(1-\tau)$ .

By deriving  $\tau W_{atm}$  from each measurement in a cooling and heating calibration period the phase lag between the cooling of the  
base and the base of the thermopile became clear. The distance between where the base temperature is measured and the base  
560 of the thermopile is about 10 mm, and during the calibration periods the delay in response of the thermopile base was found



to be about 9 s for ACP96. Including that phase lag in the linear LSQ methods improved the confidence intervals for each linear LSQ analysis by factors of 3 to over 10 but had little impact on the derived gradients and intercepts. However, it did improve the measurement estimate of  $\tau W_{atm}$  from individual measurements and provided a method to estimate the variance of  $\tau W_{atm}$  during a calibration period without need of a reference radiometer.

565 The linear LSQ method using the voltage as the predictor has significant benefits in analysing both the magnitude of components and the impact of errors in each component. This is examined below both for the impact of the Seebeck coefficient and the differences between the new Eq. (18) and Eq. (22) from Reda et al., 2012.

The comparisons between the IRIS and ACP irradiances in the results above suggest that the ACP thermopile is stable over time from hours to months and producing irradiance ratios to a reference within 2% over 2020 and with maximum differences  
570 of  $5 \text{ Wm}^{-2}$ . Reda et al., 2012 proposed that the linear LSQ  $\langle C \rangle$  value from a single linear LSQ calibration period be used as the valid C for the period between the end of the heating period that generated the linear LSQ value until the next LSQ calibration period usually within a couple of hours. The results from Reda et al., 2012 and the results presented above for ACP96 suggest that during a single night of linear LSQ calibrations the derived  $\langle C \rangle$  can vary by more than  $\pm 5\%$  of C yet the  
575 typical F3 thermopile is found to be stable well within  $\pm 2\%$  over years for both solar and IR measurements. In other radiometric linear LSQ calibration methods mean or mode statistics of several linear LSQ calibrations is typically used to reduce uncertainty in calibrations on the assumption that the value is a constant in time. The results above support using a value that represents a mean or mode resulting from at least 20 calibration periods spread over several nights in low water vapour content conditions.

### 9.1 Uncertainty in the Seebeck coefficient using linear LSQ

580 The Reda et al., 2012 and the new equation are dependent on the estimate of the Seebeck coefficient  $S$  in Eq. (7). A fixed value of  $7.044 \cdot 10^{-4}$  was used in the analysis above. In steady state conditions when measuring the incoming irradiance, the impact of any offset from the true value is likely minor provided the other coefficients in new equation are known.

The Seebeck coefficient has direct influence in both the  $W_r$  term and the  $(T_r - T_c)$  term of the new equation. For the  $(T_r - T_c)$  term the impact is straight forward given Eq. (7) in that if the error in the Seebeck coefficient is  $\Delta S$  then the contributory error is  
585  $\Delta S \gamma$  for  $\langle K_1 \rangle$  and  $\langle \tau W_{atm} \rangle$ . The impact of any error in  $S$  is slightly more complicated for  $W_r$  but the ACP96 2020 data suggest similar impacts. This is shown in Figure 10 plotting the difference in  $\langle K_1 \rangle$  when ignoring  $S$  in the  $\langle A_r \rangle$  term. The difference was calculated by subtracting the receiver slope assuming  $S=0$ , that is base irradiance slope  $\langle A_b \rangle$ , from the slope derived using  $S$ . The difference changes through the year inversely to the magnitude to the base temperature, but on average is  $\sim -0.0033$  or about  $-4\%$  of  $\langle K_1 \rangle$  which implies a 25% error in  $S$  has an impact of 1% on  $\langle K_1 \rangle$ .

590 For the Reda et al., 2012 equation the impact of the Seebeck coefficient is nearly doubled as the scaling factor is  $(2 - \varepsilon_c)$  instead of 1 for the new equation.

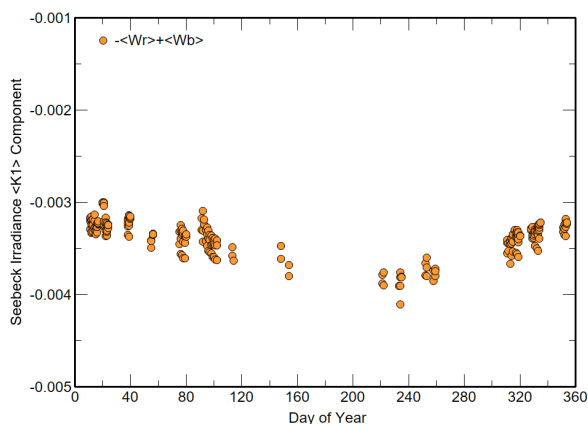
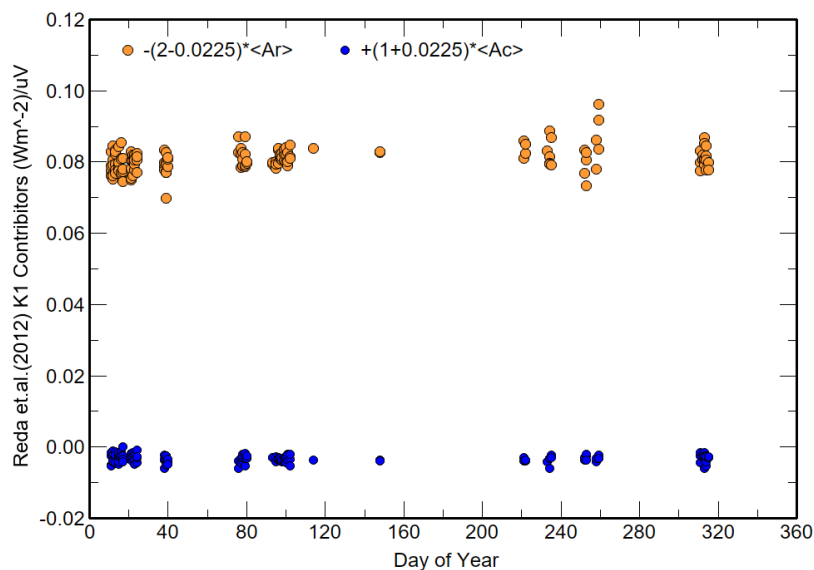


**Figure 10.** The difference in the receiver irradiance slope  $\langle A_r \rangle$  and the slope by assuming the Seebeck coefficient is zero  $\langle A_b \rangle$  when deriving  $\langle K_1 \rangle$  from the linear LSQ slope.

595 **9.2 Comparing  $\langle C \rangle$  and  $\langle \tau W_{atm} \rangle$  using the Reda et al., 2012 equation and the new equation.**

Isolating the coefficients that impact on the derived  $\langle K_I \rangle$  via linear LSQ also allows the calculation of the  $\langle K_I \rangle$  value based on the Reda et al., 2012 equation. Figure 11 shows the two components in Eq. (22) after applying the scaling factors to generate  $\langle K_I \rangle$ ; in essence  $W_r$  dominates the calculation with a small negative contribution from  $W_c$ .



600 **Figure 11.** The two slope contributions to  $\langle K_I \rangle$  for the equation developed by Reda et al., 2012.



605

The differences between the derived  $\langle C \rangle$  for both the new and Reda et al., 2012 equations by linear LSQ are shown in figure 12 and for  $\langle W_{atm} \rangle$  in figure 13. The different types of  $\langle C \rangle$  are separated by about  $2.5 \text{ uV}/(\text{Wm}^{-2})$  with the Reda et al., 2012 values being higher. The  $\langle W_{atm} \rangle$  differences between IRIS4 and Reda et al., 2012 equation were between  $\pm 12 \text{ Wm}^{-2}$ , while the differences to the new equation are bounded by  $+4$  and  $-8 \text{ Wm}^{-2}$  about half the range of the Reda et al., 2012 equation

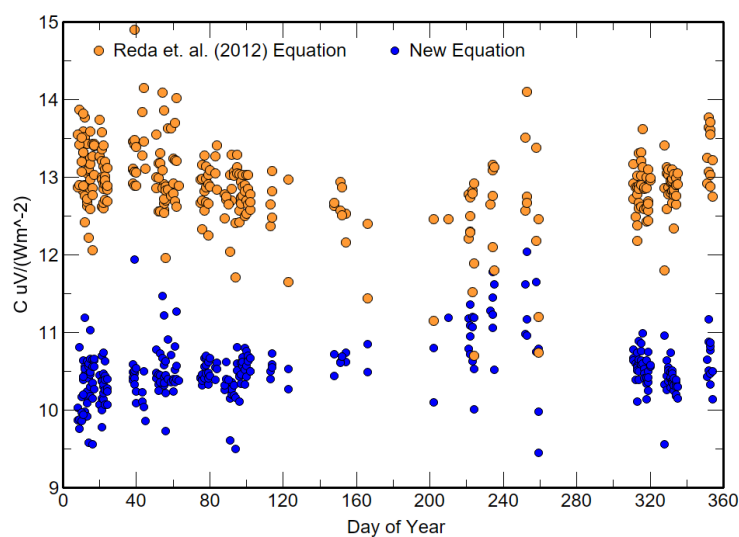
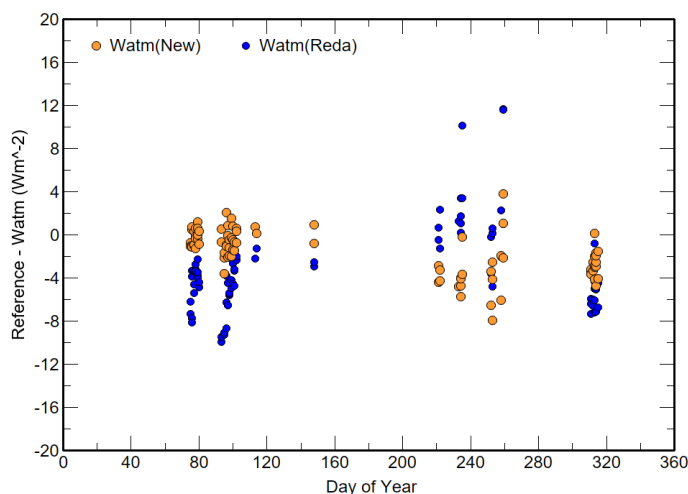


**Figure 12.** The derived  $C$  values derived from 244 linear LSQ calibration in 2020 for the Reda et al., 2012 and new equation using and concentrator emissivity of 0.0225 for both and a convection coefficient of 6.5 for the new equation.





610 **Figure 13: The comparison of  $\langle W_{am} \rangle$  derived from the new and Reda et al., 2012 equations to the mean IRIS4 irradiances for each linear LSQ calibration period in 2020.**

### 9.3 Uncertainties in concentrator emissivity and convection coefficient

The concentrator emissivity  $\varepsilon_c$  used in this study was 0.0225 as derived for ACP95 by NIST and reported by Reda et al., 2012. If  $\varepsilon_c$  is in error by  $\Delta\varepsilon_c$  it may be evident by comparing the mean differences ( $W_{ref} - W_{ACP}$ ) for different  $W_{ref}$ . As  $W_{ref}$  increases  
615 the difference ( $W_{ref} - W_{ACP}$ ) will be proportional to  $(-\Delta\varepsilon_c W_{ref})$  but this is complicated by needing to divide by the transmission. The comparison data with IRIS4 was examined to see if a significant trend could be found by using various estimates of  $\varepsilon_c$  but results were well below the noise of the derived components and  $C$ .

To remove the influence of  $C$  the relationship between ( $W_{IRIS4} - W_{ACP96}$ ) and  $W_c$  was calculated for 2 thermopile voltage ranges of  $[-850 \mu\text{V}, -800 \mu\text{V}]$  and  $[-800 \mu\text{V}, -750 \mu\text{V}]$  using IRIS4 irradiances as the reference. The results were inconclusive with  
620 the new equation the typical range of  $W_{IRIS4} - W_{ACP96}$  was  $\pm 2 \text{ Wm}^{-2}$  over a range  $\Delta W_c$  of  $125 \text{ Wm}^{-2}$  and using values of  $\varepsilon_c$  in the range (0.020, 0.030). However, the smallest rates of change were for a concentrator emissivity 0.020, which is within 0.001 of the nominal value for the emissivity of polished gold. A concentrator emissivity  $\varepsilon_c$  of 0.0225 is therefore a reasonable assumption until an independent method of determining the concentrator emissivity has been developed.

Incorrect assignment of the convection coefficient  $\gamma$  has different impacts depending on the calibration methodology when  
625 using the new equation; there is no impact on the Reda et al., 2012 equation as convection is not considered explicitly. A 25% offset in  $\gamma$  is likely to introduce a small  $2.0 \text{ Wm}^{-2}$  offset or less using the new equation in steady state or passive measurement conditions as shown in Table 3 and 4. However, for perturbed conditions, as in the linear LSQ method where the base of the ACP is cooled in a few minutes, an offset error of 25% in  $\gamma$  will cause a significant offsets in the derived  $C$ , and large offsets between the derived  $W_{am}$  and measurements from reference instruments as shown in Table 5 and 6. The linear LSQ results  
630 above provided a representative value for  $\gamma$  but only by comparison to a reference instrument, which then negates the independence of the ACP as a reference irradiance.

The convection coefficient of air is dependent on water vapour with higher content giving a higher coefficient. The initial investigations reported above suggest that for an ACP to be a primary standard via the linear LSQ method more investigation is required to determine either the value of  $\gamma$  for specific water vapour content or a maximum water vapour content for suitable  
635 linear LSQ, and most importantly the impact of assuming it is constant during the LSQ method. In periods of high relative humidity it is highly likely that the convection coefficient may not be constant during the cooling-heating period and is responsible for the remaining sinusoidal variations found in 2020.

The solar calibration method is also dependent on a reference radiometer with a low uncertainty. However, it can provide an estimate of  $C$  within uncertainty of the assumed emissivity of Parsons Black. With a new F3 thermopile those emissivity  
640 uncertainties should be small, and hence would provide likely uncertainty limits for  $C$  independent of the linear LSQ calibration



method. Moreover, a regular, say annual, sequence of solar calibration would provide an independent assessment of the stability of  $C$  without assumptions involving concentrator emissivity and transmission and convection. Using this solar-derived value of  $C$  and given the significant contribution the convection term makes to the linear LSQ method derivation of  $\langle C \rangle$ , the solar calibration could be used to solve for the convection coefficient  $\gamma$  for an assumed value of concentrator emissivity.

645 For the Reda et al., 2012 and new equations, the use either a reference irradiance or black body irradiance ( $W_{BB}$ ) to calibrate an ACP is problematic as the predictand irradiance components  $V$ ,  $W_r$ ,  $W_c$  and  $(T_r - T_c)$  or  $(W_r - W_c)$  are all highly correlated, making it difficult to solve with standard polynomial regression techniques. While a blackbody calibration can ensure a constant incoming irradiance, providing a useful  $T_{air}$  or an appropriate analogy via  $T_c$  has yet to be achieved if  $T_c$  is significantly different from the irradiance source eg. a blackbody or cold sky. Hence work in further characterising an ACP and its key  
650 parameters in different environments needs to be done.

The new equation was developed applying Kirchhoff's law of radiative transfer for radiative transfer in air. For the solar calibration method and the calibration using a reference irradiance, the ACP is essentially in steady state, while in the linear LSQ method the ACP is in a transient mode. Kirchhoff's law only applies in periods of radiative equilibrium. Further work is required to ensure that confirms the ACP is still in radiative equilibrium during the cooling-heating cycle.

## 655 **10 Conclusions**

The new equation for an ACP derived from the application of Kirchhoff's law and inclusion of a convection term provided irradiances agreeing well with measurements from two reference IR radiometers over 11 months in 2020 assuming either a solar derived calibration or minimization method using a reference irradiance.

The new equation was adapted to the linear LSQ method of Reda et al., 2012 for solving for  $K_1$  (or  $C$ ). Given the only LSQ  
660 predictor was the thermopile voltage the method was extended to determine the 5 linear components independently of the equations and given their linear relationship to the voltage combined for both the new and Reda et al., 2012 equations. This also provided an estimate of the relative contribution of each component to the calibration values.

The linear LSQ results indicated that the new equation irradiances were for most cases more consistent with the two reference radiometer irradiances, but that consistency was dependent on the value of the convection coefficient. A method of examining  
665 the convection coefficient independent of a reference irradiance was developed by solving for  $\tau W_{am}$  during cooling and heating periods and highlighted  $\sim 9$  s time lag between the representative voltage for the body and concentrator temperature measurements. When the lag was incorporated into the linear LSQ method the confidence intervals for all slope quantities improved significantly and sinusoidal variations in the derived irradiance during a heating cooling period were reduced but not eliminate. However, a solar or blackbody estimation process to determine the convection coefficient for linear LSQ  
670 conditions is yet to be developed.



Further work could include modifications of the ACP to reduce the impact of the convection term during LSQ calibrations. For example, reducing the water vapour content in the ACP through weak flushing of body and concentrator with dry air and minimising the temperature difference between the concentrator and body temperature.

675 Via the linear LSQ method an estimate for the concentrator transmission can also be obtained using a reference terrestrial irradiance. However, the preferred method should be laboratory measurements as performed by Jinan et al., 2010 but using the new equation rather than assuming the measurements are performed in a vacuum.

680 A solar calibration of future ACP thermopiles is recommended provided the thermopile has not been subjected to solar irradiance for extended periods over several years. The solar calibration will produce an estimate of  $C$  that will be close to the maximum possible for the thermopile and thus provide either an independent estimate of  $C$  or periodically provide a mechanism to independently assess the long-term stability of the ACP thermopile responsivity.

The new equation was developed applying Kirchhoff's law of radiative transfer for radiative transfer in air. For the solar calibration method and the calibrations using a reference irradiance, the ACP is essentially in steady state, while in the linear LSQ method the ACP is in a transient mode. Kirchhoff's law only applies in periods of radiative equilibrium, hence further work is required to confirm that during the cooling-heating cycle the ACP remains in radiative equilibrium.

## 685 **References**

- Gröbner, J.: A transfer standard radiometer for atmospheric longwave irradiance measurements, *Metrologia*, 49, 105-111, 2012.
- Gröbner, J. and Wacker S.: Pyrgometer calibration procedure at the WRC/PMOD-IRC, WMO, Instrument and Observing Report 120, pp13, 2012.
- 690 Gröbner, J., Investigation of ACP96 at PMOD/WRC, [doi.org/10.5281/zenodo.7047680](https://doi.org/10.5281/zenodo.7047680), 2021.
- Jinan, Z., Hanssen L., Reda I., Scheuch J.: Preliminary characterization study of a gold-plated concentrator for hemispherical longwave irradiance measurements. Paper no 77920Z. Proceedings of SPIE Conference -3-5 Aug 2010, San Diego Volume 7792. 2010.
- Kondratyev, Y. A.: Radiation in the Atmosphere. Academic Press, International Physics Series, Vol 12, pp 912, 1969.
- 695 Philipona, R., Frohlich C., Betz C.: Characterization of pyrgeometers and the accuracy of atmospheric long-wave radiation measurements, *Appl. Opt.*, 34(9), 1598–1605, 1995.
- Pascoe, D. and Forgan B. W.:(1980) An investigation of the Linke-Feussner pyrheliometer temperature coefficient, *Solar Energy*, 25, 191-192, 1980.
- Robinson, G. D.: *Solar Radiation*, Elsevier, pp269, 1966.



- 700 Reda, I., Jinan Z., Hanssen L., Wilthan B., Myers D., T. Stoffel T.: An absolute cavity pyrgeometer to measure the absolute outdoor longwave irradiance with traceability to international system of units, SI. *Jnl Atmos. Solar-Terrestrial Physics*, 77, 132-143, 2012
- Vignola, F., Michalsky J., T. Stoffel T.: *Solar and infrared radiation measurements*. CRC Press, ISBN 978-1-4398-5189-0, 2012.